

# Design of High Sensitivity, High Resolution Compact Single Photon Imaging Devices for Small Animal and Dedicated Breast Imaging

Mark F. Smith, *Member, IEEE*, Stan Majewski, Steven R. Meikle, Andrew G. Weisenberger, Vladimir Popov, Randolph F. Wojcik

**Abstract**— Imaging the biodistribution of single photon emitting radiotracers in small animals and in the breast with high resolution and high sensitivity is an important challenge. Recent work has shown that single photon emission computed tomography (SPECT) imaging of small objects with coded aperture collimators and iterative image reconstruction may provide an order of magnitude increase in sensitivity yet maintain high spatial resolution. We propose a new system design with compact detectors for single photon small animal and breast imaging. Key features are 1) multipinhole masks for improved sensitivity, 2) pixellated NaI(Tl) scintillator arrays with small crystals for high resolution and 3) flat panel or flangeless compact position sensitive photomultiplier tubes. Analyses for a multipinhole small animal device with four 10 cm x 20 cm detectors and 1.5 mm detector resolution indicate that 0.9-1.3 mm resolution in image space could be achieved for 0.5-0.8 mm diameter pinholes with geometric sensitivity of 0.2-0.6%, where a point in the brain is imaged through 20 pinholes/mask. A design for a multipinhole breast imager incorporates 20 cm x 20 cm pixellated detectors and lower magnification. Predicted image resolution in the center of the field of view is 1.9 mm for 0.8 mm pinholes, with sensitivity of about 0.045% in the center of the field of view for breast tissue imaged through 20 pinholes/mask. Additional modeling, iterative image reconstruction, device component and phantom tests are desirable to optimize device specifications.

## I. INTRODUCTION

The design of high sensitivity, high resolution detectors for single photon imaging in biomedicine is an important challenge. One area where such detectors would be beneficial is functional small animal imaging, where potential applications include investigations of metabolism, tissue viability and receptor and gene expression. Longitudinal *in vivo* studies with single photon-emitting radiopharmaceuticals using these detectors would be valuable in drug discovery and development. Detectors with high resolution

and high sensitivity are also of great interest for human studies of organs such as the breast, where increased uptake of single photon tracers such as Tc-99m sestamibi has been reported in carcinomas [1].

Pinhole single photon emission computed tomography (SPECT) has been investigated for small animal imaging due to its potential for high resolution achieved through object magnification. Single pinhole imaging for small animals has been investigated by many research groups [2-11] and pinhole collimation has been used with pixellated detectors in a commercially available system [12]. Pinhole SPECT and PET for high resolution small animal imaging have recently been reviewed [13].

Multiple pinhole coded aperture systems have been studied for brain imaging [14, 15] and are being further considered for high resolution imaging of small objects [16] and small animals [17, 18]. A multipinhole, focused collimator has been proposed for small animal brain imaging [19]. Iterative methods are being used for three-dimensional image reconstruction where projection data from multiple pinholes or coded apertures overlap.

The same features that make pinhole collimation attractive for small animal imaging also apply to scintimammographic imaging, though there has been less research for this application. There have been initial studies of pinhole collimation for high resolution planar scintimammography [20] and tomographic breast imaging [21].

There are several challenges in the design of high sensitivity, high resolution compact detectors for small animal and dedicated breast imaging. In this contribution we will investigate tradeoffs between sensitivity and resolution in pinhole aperture design and between image resolution and object magnification in choosing the focal length for pinhole collimation. A methodology for choosing the placement of pinholes in a multipinhole mask will be presented. A design for compact, pixellated detectors will be presented, with attention given to the scintillator material, crystal size, overall array size, light guides, photomultiplier tubes and data acquisition system. Though small animal and breast imaging applications are considered, device design for small animal imaging will be more fully developed.

---

M. F. Smith (telephone 757-269-5539, e-mail: mfsmith@jlab.org), S. Majewski, A. G. Weisenberger, V. Popov and R. F. Wojcik are with the Thomas Jefferson National Accelerator Facility (Jefferson Lab), Newport News, VA 23606 USA.

S. R. Meikle is with the Department of PET and Nuclear Medicine, Royal Prince Alfred Hospital, Sydney, Australia.

The Southeastern Universities Research Association (SURA) operates the Thomas Jefferson National Accelerator Facility for the United States Department of Energy under contract DE-AC05-84ER40150. This work is supported by the Office of Biological and Environmental Research of the Office of Science of the U.S. Department of Energy.

## II. IMAGING SYSTEM DESIGN

### A. Multipinhole Mask Design and Detector Configuration for Small Animal Imaging

The resolution and sensitivity of a small animal imaging device built with a multipinhole array is dependent on several factors, including the pinhole size, the distance of the pinholes or array openings from the object and the size of the detector array. Estimates of design tradeoffs can be made using formulas developed for single pinhole imaging [22] and generalized to the multipinhole case. The assumption is made, as for single pinhole SPECT design, that the resolution from tomographic reconstruction in image space will be approximately the same as that derived from planar image analysis.

Plots of resolution in image space were made as a function of object magnification and different pinhole sizes for a detector with 1.5 mm resolution (Figure 1a). For small animal imaging 1.25 mm image resolution can be achieved for magnifications of 3-4 and pinhole diameters less than 0.9 mm.

The target organ for our small animal imaging application is the mouse brain, which can be modeled for detector design purposes as a 12 mm long, 8 mm diameter cylinder. A small animal SPECT system was designed with the center of a 3 cm diameter cylindrical mouse burrow located 2 cm from the multipinhole mask (Figure 2). The focal length is 7 cm and so magnification is 3.5 for a point in the brain on the axis of rotation at the center of the burrow. A target image resolution of approximately 1 mm can be achieved with a pinhole diameter of 0.7 mm (Figure 1a). The proposed system would have 4 detectors and associated multipinhole collimators spaced at 90 degree intervals around the animal. The detectors and collimators will be rotated for complete angular sampling. The detectors extend axially so that the entire animal could be imaged on a 10 cm wide x 20 cm long scintillator array.

A novel aspect of the multipinhole collimator design is that the placement of the pinholes on the aperture masks can be chosen by 1) specifying the locations of the magnified brain images on the detector, then 2) backprojecting these brain images to find the corresponding pinhole center positions on the masks. In this way the amount of brain overlap (multiplexing) on the detector can be used as a parameter in mask design. For the system geometry of Figure 2 and pinhole spacing of 12 mm axially and 7 mm transaxially there will be no overlap of brain images on the detector. This spacing corresponds to a 55 pinhole configuration for a 4 cm x 14 cm multipinhole mask (Figure 3c). With a denser 127 pinhole mask (Figure 3d) there will be brain image overlap (Figure 4).

Estimates of system sensitivity vs. resolution were made for prototype devices with four detectors and assuming that a point in the brain projects through 20 pinholes (Figure 1b). These sensitivity factors can be scaled to reflect different pinhole densities. Based on these resolution and sensitivity calculations, we have chosen to use a 0.7 mm diameter

pinhole (Figure 5) and we are fabricating a series of masks with different numbers of pinholes (Figure 3). The masks are 5 mm thick tungsten and are designed for Tc-99m imaging.

Image reconstruction will be performed using iterative methods, for which the resolution and the signal-to-noise ratio vary with iteration. Our objective is to characterize resolution/signal-to-noise/sensitivity tradeoffs for these masks, which have different amounts of multiplexing of projection data. The overlap of body tissue activity with brain activity will make brain activity estimation more difficult, though the limited acceptance angle of the pinhole apertures will prevent overlap of activity from some organs at the posterior of the small animal.

### B. Multipinhole Mask Design and Detector Configuration for Breast Imaging

The approach to the design of a multipinhole imaging system for the breast is similar to that for small animals. Due to the larger size of the breast and a desire to limit the breast detector size to 20 cm x 20 cm, magnification cannot be as great as for small animals. This leads to a more modest target image resolution, on the order of 1.5-2.0 mm, which would represent an important step in imaging smaller breast carcinomas (Figure 6a).

For dedicated breast imaging larger multipinhole masks (15 cm x 15 cm) and detector heads (20 cm x 20 cm) are proposed (Figure 7). If the masks are located 7.5 cm from the axis of rotation (AOR), forming a square around the breast, and the focal length is 9 cm, then magnification for a point on the axis of rotation is 1.2. With 0.8 mm pinholes the predicted resolution on the AOR is 1.9 mm (Figure 6b) and geometric sensitivity on the AOR is 0.045% for a point in the breast imaged through 20 pinholes. Sensitivity is not as great as for a small animal because of the larger breast size and a larger average distance between the pinhole collimators and the imaged breast tissue.

### C. Detector Head Design

#### 1) Scintillator Arrays

The scintillator arrays will be made from  $1 \times 1 \times 5 \text{ mm}^3$  or  $1.25 \times 1.25 \times 10 \text{ mm}^3$  NaI(Tl) crystals, with step sizes of 1.25 mm or 1.5 mm, respectively. This new scintillator technology was very recently made available from Saint-Gobain Crystals and Detectors (formerly Bicon, Inc.). We will consult with Saint-Gobain to determine optimized scintillator array parameters. The proposed active area of the detector heads is 10 cm x 20 cm for small animal imaging and 20 cm x 20 cm for dedicated breast imaging.

#### 2) Position Sensitive Photomultiplier Tubes (PSPMTs)

The unique detector technology to be utilized in the proposed SPECT imagers is based on an array of the new flat panel PSPMTs, if available. These offer a more uniform spatial response due to decreased dead space near the edges. An alternative is the use of the presently available latest generation flangeless compact Hamamatsu R8520-00-C12 PSPMTs. The PSPMTs will be arranged in 4x8 arrays (small animal imager) or 8x8 arrays (breast imager) to form single

detector heads (Figure 8). This photomultiplier technology is very reliable and offers the opportunity to build compact, stable and robust imaging heads. The planned PSPMT spacing is 26.14 mm center-to-center with an active photocathode size of 22 mm square. Hamamatsu has indicated that a new 24 mm square version will soon be available, which will aid in imaging crystal array elements in the gap between PSPMTs.

### 3) Light Guides

The current solution for an optimized light guide is to use two separate optical parts to efficiently collect light from any pixel in the scintillator array. A flat "spreader" window is 4.5 mm thick and facilitates the spreading of the scintillation light cones away from dead regions along crack lines between the PSPMTs. The optical trapezoid light collectors are 4.5 mm thick and have 26.14 mm square input size (physical size of the PSPMT) and a 21 mm square output side to couple to the PMT window to match the photocathode size. The trapezoids direct light from the pixels placed above dead edge regions between PSPMTs towards PSPMT centers. In extensive laboratory tests this simple light guide arrangement produced very uniform response across the detector surface.

### 4) Advanced Detector Acquisition System

The detector will be operated with a high-rate data acquisition system built at Jefferson Lab and interfaced via high speed Ethernet to a desktop computer running reconstruction and imaging software. User interface and image display will be handled by control software developed with the Kmax 7.0 package (Sparrow Corporation, Daytona Beach, FL) installed on an Apple Macintosh G4 computer.

For each detector head we will use a custom-designed electronically truncated centroid readout method to facilitate the digitization of the anode charge pulses from the cross-wired anodes of the PSPMTs. The R8520-00-C12 PSPMTs have 6(x)x6(y) anode wire readout. Jefferson Lab, in collaboration with Sparrow, has been developing a high performance fast VME-based data acquisition system using a Motorola MVME2700-1431 VME 366MHz G3 CPU. The analog channels of the detector are read using the CAEN Inc. (Viareggio, Italy) V785 32 channel ADC VME board, which is able to sample all channels simultaneously with 12 bit resolution at a conversion speed of 1 sample/6 microseconds. The VME CPU manages the data processing and provides image data to the Macintosh workstation. A schematic diagram of the data acquisition system is displayed in Figure 9.

## III. DISCUSSION

The resolution analyses did not consider depth of interaction effects in the scintillation crystals, which will cause some degradation of image resolution. Multiplexing of images on the detector will affect signal-to-noise ratios and reconstructed image resolution and is a critical factor that needs to be investigated. A key consideration is whether higher spatial frequencies can be recovered with increasing iteration number before the signal-to-noise ratio degrades the

reconstructed images too severely. Numerical simulations of mouse and breast phantoms, as well as experiments with physical mouse and breast phantoms, will be used to investigate these factors.

## IV. CONCLUSIONS

A new design has been proposed for high sensitivity, high resolution detector systems for single photon small animal and breast imaging. Sensitivity is increased through the use of multipinhole masks. A key feature of multipinhole mask design for small animal imaging is that the masks are designed with different overlap (multiplexing) of the mouse brain projections on the detector. The imaging system is designed with compact, pixellated detectors and flat panel PSPMTs. Additional modeling, iterative image reconstruction, device component and phantom tests are desirable to optimize device specifications prior to small animal or clinical breast imaging.

## V. REFERENCES

- [1] I. Khalkhali, J. Cutrone, I. Mena, L. Diggles, R. Venegas, H. Vargas, B. Jackson, and S. Klein, "Technetium-99m-sestamibi scintimammography of breast lesions: clinical and pathological follow-up," *J. Nucl. Med.*, vol. 36, pp. 1784-1789, 1995.
- [2] S.-E. Strand, M. Ivanovic, K. Erlandsson, D. Franceschi, T. Button, K. Sjogren, and D. A. Weber, "Small animal imaging with pinhole single-photon emission computed tomography," *Cancer*, vol. 73 (suppl), pp. 981-984, 1994.
- [3] D. A. Weber, M. Ivanovic, D. Franceschi, S.-E. Strand, K. Erlandsson, M. Franceschi, H. L. Atkins, J. A. Coderre, H. Susskind, T. Button, and K. Ljunggren, "Pinhole SPECT: an approach to *in vivo* high resolution SPECT imaging in small laboratory animals," *J. Nucl. Med.*, vol. 35, pp. 342-348, 1994.
- [4] R. J. Jaszczak, J. Li, H. Wang, M. R. Zalutsky, and R. E. Coleman, "Pinhole collimation for ultra-high-resolution, small-field-of-view SPECT," *Phys. Med. Biol.*, vol. 39, pp. 425-437, 1994.
- [5] K. Ishizu, T. Mukai, Y. Yonekura, M. Pagani, T. Fujita, Y. Magata, S. Nishizawa, N. Tamaki, H. Shibasaki, and J. Konishi, "Ultra-high resolution SPECT system using four pinhole collimators for small animal studies," *J. Nucl. Med.*, vol. 36, pp. 2282-2287, 1995.
- [6] K. Ogawa, T. Kawade, K. Nakamura, A. Kubo, and T. Ichihara, "Ultra high resolution pinhole SPECT for small animal study," *IEEE Trans. Nucl. Sci.*, vol. 45, pp. 3122-3126, 1998.
- [7] M. C. Wu, H. R. Tang, J. W. O'Connell, D. W. Gao, A. Ido, A. J. Da Silva, K. Iwata, B. H. Hasegawa, and M. W. Dae, "An ultra high resolution ECG-gated myocardial imaging system for small animals," *IEEE Trans. Nucl. Sci.*, vol. 46, pp. 1199-1202, 1999.
- [8] N. Schramm, A. Wirrwar, F. Sonnenberg, and H. Halling, "Compact high resolution detector for small animal SPECT," *IEEE Trans. Nucl. Sci.*, vol. 47, pp. 1163-1167, 2000.
- [9] B. M. W. Tsui, Y. Wang, E. C. Frey, and D. E. Wessell, "Application of an ultra high-resolution pinhole SPECT system based on a conventional camera for small animal imaging," *J. Nucl. Med.*, vol. 42, pp. 54P, 2001.
- [10] F. J. Beekman, D. P. McElroy, F. Berger, E. J. Hoffman, and S. R. Cherry, "Sub-millimeter resolution in  $^{125}\text{I}$  *in vivo* imaging in mice using micro-pinhole," *J. Nucl. Med.*, vol. 42, pp. 55P, 2001.
- [11] S. Tanada, T. Irie, N. Watanabe, H. Murata, H. Murayama, and Y. Sasaki, "Performance characteristic of small-animal dedicated SPECT system," *J. Nucl. Med.*, vol. 42, pp. 204P, 2001.
- [12] L. R. MacDonald, B. E. Patt, J. S. Iwanczyk, B. M. W. Tsui, Y. Wang, E. C. Frey, D. E. Wessell, P. D. Acton, and H. F. Kung, "Pinhole SPECT of mice using the LumaGEM gamma camera," *IEEE Trans. Nucl. Sci.*, vol. 48, pp. 830-836, 2001.
- [13] D. A. Weber and M. Ivanovic, "Ultra-high-resolution imaging of small animals: implications for preclinical and research studies," *J. Nucl. Cardiol.*, vol. 6, pp. 332-344, 1999.
- [14] R. K. Rowe, J. N. Aarsvold, H. H. Barrett, J.-C. Chen, W. P. Klein, B. A. Moore, I. W. Pang, D. D. Patton, and T. A. White, "A stationary

hemispherical SPECT imager for three-dimensional brain imaging," *J. Nucl. Med.*, vol. 34, pp. 474-480, 1993.

[15] M. M. Rogulski, H. B. Barber, H. H. Barrett, R. L. Shoemaker, and J. M. Woolfenden, "Ultra-high-resolution brain SPECT imaging: simulation results," *IEEE Trans. Nucl. Sci.*, vol. 40, pp. 1123-1129, 1993.

[16] D. W. Wilson, H. H. Barrett, and E. W. Clarkson, "Reconstruction of two- and three-dimensional images from synthetic-collimator data," *IEEE Trans. Med. Imaging*, vol. 19, pp. 412-422, 2000.

[17] S. R. Meikle, R. R. Fulton, S. Eberl, M. Dahlbom, K.-P. Wong, and M. J. Fulham, "An investigation of coded aperture imaging for small animal SPECT," *IEEE Trans. Nucl. Sci.*, vol. 48, pp. 816-821, 2001.

[18] D. J. Wagenaar, J. C. Engdahl, V. Simcic, E. G. Hawman, T. Mertelmeier, U. Mahmood, R. Accorsi, and R. C. Lanza, "Use of conventional gamma cameras for small animal imaging," *Conference Record of the 2000 IEEE Nuclear Science Symposium and Medical Imaging Conference*, 2000.

[19] A. V. Ochoa, L. Ploux, R. Mastroioppo, Y. Charon, P. Lanière, L. Pinot, and L. Valentin, "An original emission tomograph for *in vivo* brain imaging of small animals," *IEEE Trans. Nucl. Sci.*, vol. 44, pp. 1533-1537, 1997.

[20] B. M. W. Tsui, D. E. Wessell, X. D. Zhao, W. T. Wang, D. P. Lewis, and E. C. Frey, "Imaging characteristics of scintimammography using parallel-hole and pinhole collimators," *IEEE Trans. Nucl. Sci.*, vol. 45, pp. 2155-2161, 1998.

[21] C. Scarfone, R. J. Jaszczak, J. Li, M. S. Soo, M. F. Smith, K. L. Greer, and R. E. Coleman, "Breast tumor imaging using incomplete circular orbit pinhole SPECT: a phantom study," *Nucl. Med. Commun.*, vol. 18, pp. 1077-1086, 1997.

[22] H. O. Anger, "Radioisotope cameras," in *Instrumentation in Nuclear Medicine*, vol. 1, G. J. Hine, Ed. New York: Academic Press, 1967, pp. 485-552.

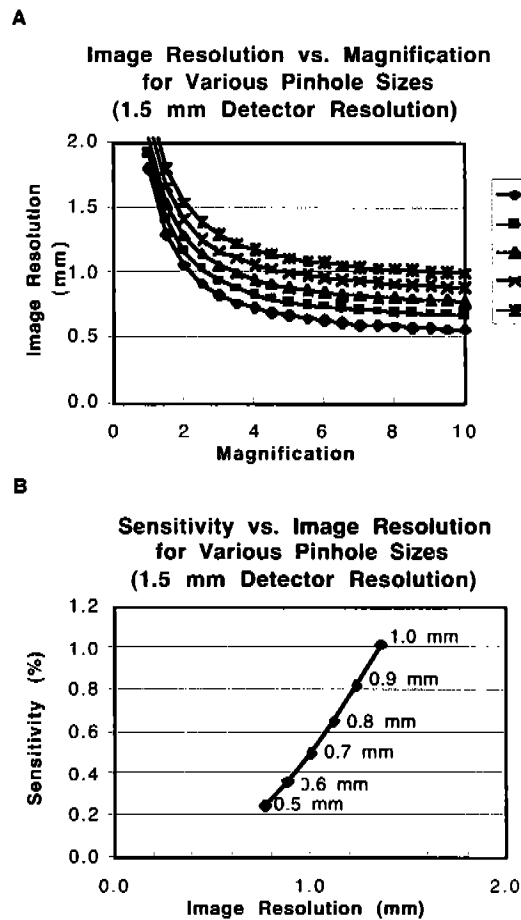


Fig. 1. For a small animal imaging device, (a) image resolution vs. magnification and (b) sensitivity vs. image resolution for various pinhole diameters and 140 keV photons. The assumption is that a point source projects through 20 pinholes for each of four detectors.

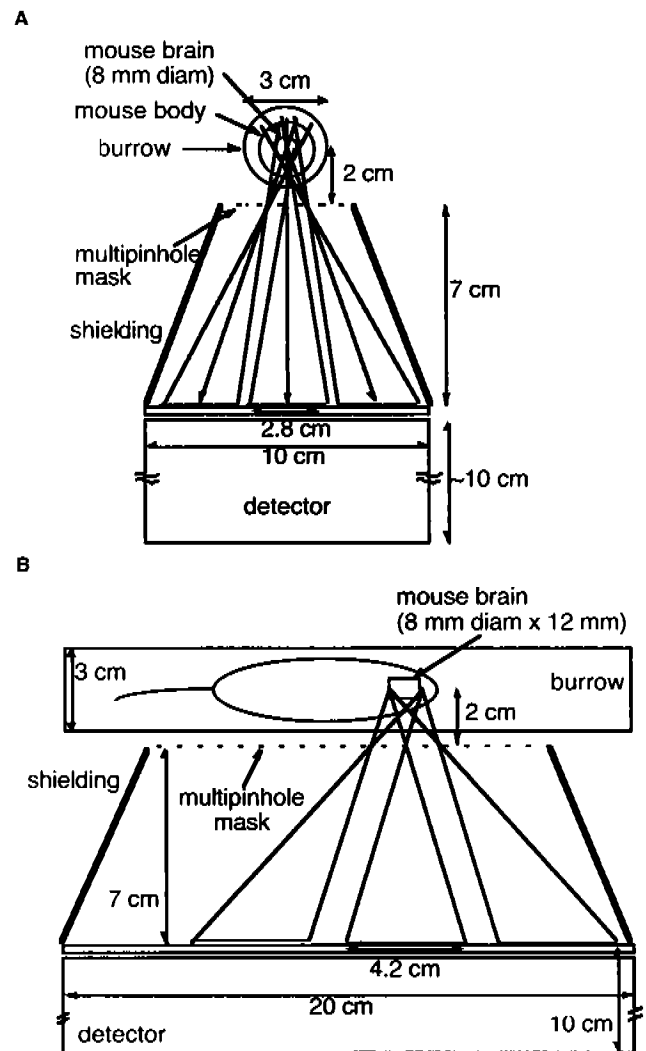


Fig. 2. Small animal system design, (a) transaxial and (b) axial views, showing one of four planned detectors. Projections of a cylinder modeling the mouse brain are shown.

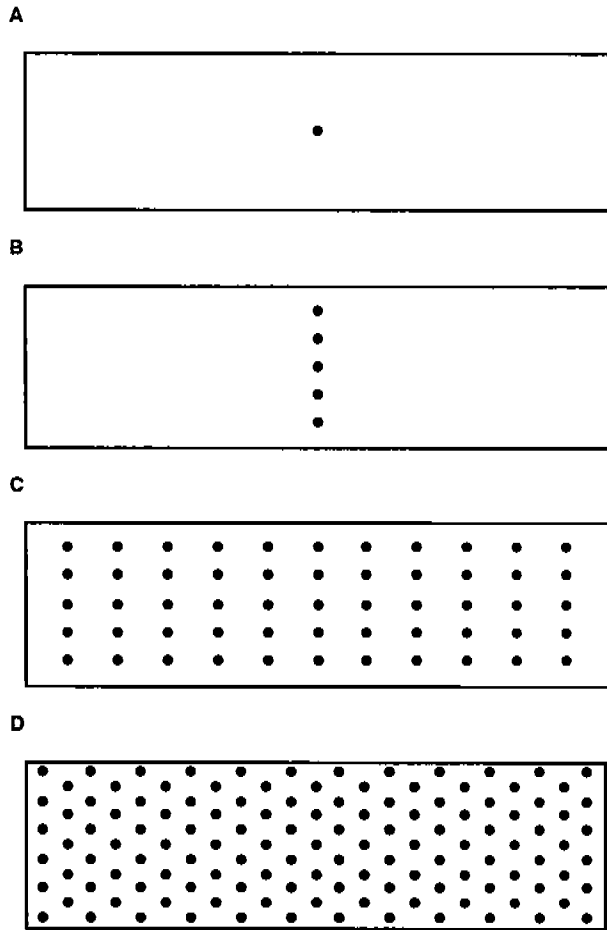


Fig. 3. Multipinhole mask designs. The centers of the apertures on the surface of the 5 mm thick masks are shown. (a) Single pinhole, (b) 5 pinholes with 7 mm spacing, (c) 55 pinholes with 12 mm axial and 7 mm transaxial spacing and (d) 127 pinholes with 6 mm between axial rows and 7 mm spacing within each axial row.

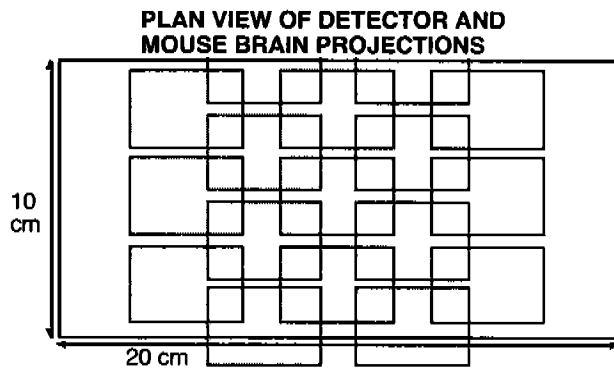


Fig. 4. Plan view of mouse brain projections on the detector head for the 127 pinhole mask of Figure 3d and the mouse brain in the center of the burrow as depicted in Figure 2.

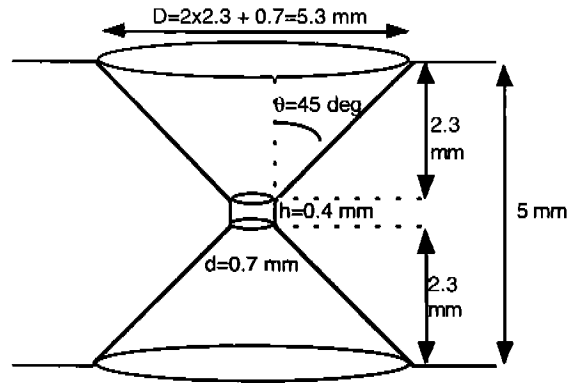


Fig. 5. Diagram of the pinhole aperture.

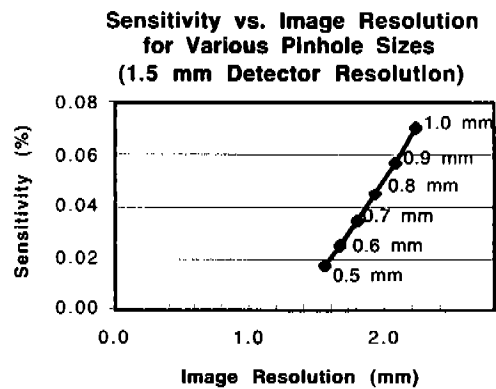
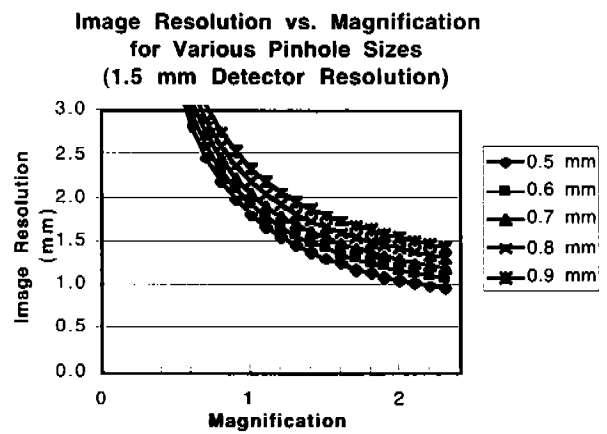


Fig. 6. For a multipinhole breast imaging device, (a) image resolution vs. magnification and (b) sensitivity vs. image resolution for various pinhole diameters and 140 keV photons. The assumption is that a point source projects through 20 pinholes for each of four detectors.

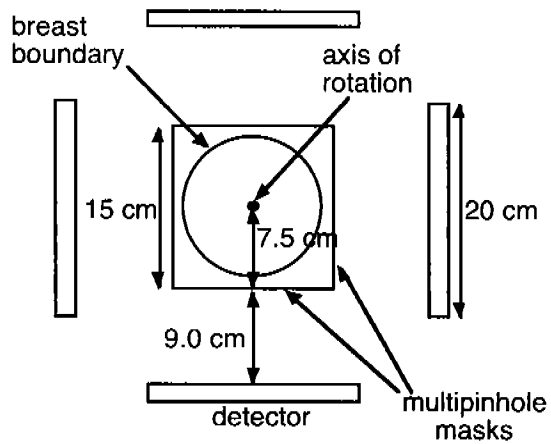


Fig. 7. Mask and detector configuration for dedicated breast imaging.

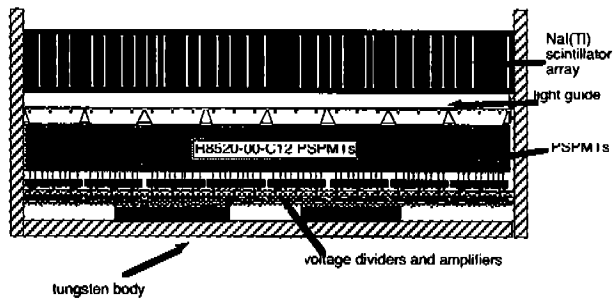


Fig. 8. Cross-section of a proposed detector head showing pixellated scintillator array, light guides, PSPMTs and front-end electronics.

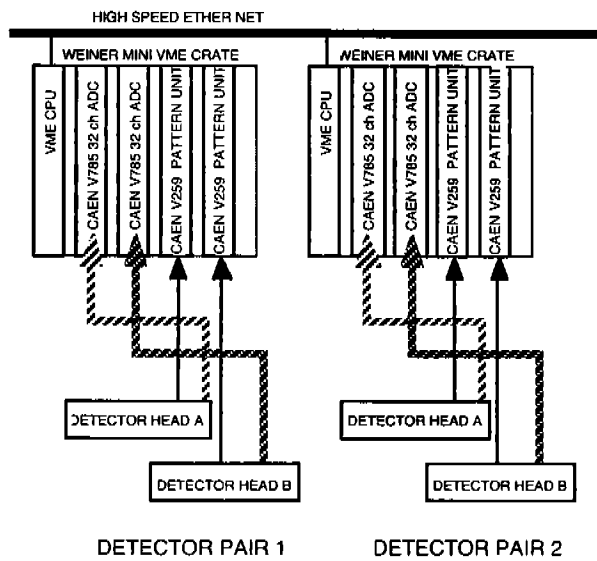


Fig. 9. Schematic diagram of the data acquisition system.